JOURNAL OF MATERIALS SCIENCE 21 (1986) 1321–1328

Mechanical property changes in sapphire by nickel ion implantation and their dependence on implantation temperature

T. HIOKI, A. ITOH, M. OHKUBO, S. NODA, H. DOI, J. KAWAMOTO, O. KAMIGAITO
Toyota Central Research and Development Laboratories, Inc., Nagakute, Aichi-gun, Aichi 480-11, Japan

Sapphire plates, cut parallel to an {0 0 0 1} plane, have been implanted with 300 keV nickel ions to doses ranging from 5×10^{12} to 1×10^{17} Ni cm^{-2} at specimen temperatures of 100, 300 and 523 K, in order to investigate the effect of implantation temperature on the mechanical property changes in sapphire caused by ion implantation. The measured changes in surface hardness, surface fracture toughness and bulk flexural strength were found to depend strongly on the implantation temperature, and were largely correlated with the residual surface compressive stress measured by using a cantilever beam technique. The surface amorphization that occurred only by the implantation at 100 K and at doses larger than $\sim 2 \times 10^{15}$ Ni cm^{-2} reduced the hardness to ~ 0.6 relative to the value of the unimplanted sapphire, and considerably increased the surface plasticity. Furthermore, the amorphization was found to involve a large volume expansion of $\sim 30\%$ and to change drastically the apparent shape and size of a Knoop indentation flaw made prior to implantation. This effect was suggested to reduce stress concentrations at surface flaws and hence to increase the flexural strength.

1. Introduction

Surface alteration of ceramic materials by ion implantation has recently been studied by an increasing number of investigators in an attempt to improve mechanical properties; the effects of ion implantation and subsequent thermal annealing on surface hardness, surface fracture-toughness and bulk fracture-stress have been investigated for α-Al_2O_3 [1–8], SiC [9–11], ZrO_2 [12–14] and MgO [15]. Ion implantation can introduce a controlled amount of alloying element in ceramics, but it also produces a large number of lattice defects. The latter effect, i.e. radiation damage, has been reported to considerably affect the mechanical properties of a ceramic particularly in its as-implanted state. It generally results in a hardness increase, i.e. radiation hardening. It also causes a volume change of the damaged region and yields a residual stress in the surface layer [16]. For single-crystal α-Al_2O_3 (sapphire), increases in bulk flexural strength and surface fracture-toughness by ion implantation have been attributed to the residual surface compressive stress [5, 6]. Furthermore, the accumulation of lattice defects with increasing ion dose eventually turns the surface layer amorphous, and the amorphization results in a reduction of hardness [6, 8–10].

The extent of radiation damage and the resulting changes in mechanical properties are expected to depend on the specimen temperature during implantation, even if other implantation conditions are fixed. In this paper, we report the results of systematic measurements on the mechanical property changes in sapphire caused by implanting nickel ions at different specimen temperatures. The measured changes in surface hardness, surface fracture-toughness and bulk flexural strength are discussed in correlation with the results on surface structure obtained by using the Rutherford-backscattering (RBS) and ion channelling (RBS/channelling), the surface profilometry and the cantilever beam techniques.

2. Experimental details

High purity (99.99% up) sapphire plates, cut parallel to the {0 0 0 1} plane, were polished to a mirror finish and annealed at 1500° C for 6 h in air. The plates were mounted on a temperature-variable specimen-holder, and were implanted with 300 keV nickel ions by using a 400 kV Cockcroft-type ion accelerator. The implantations were carried out in a vacuum of 5×10^{-5} Pa and at specimen temperatures of 100, 300 and 523 K. The ion doses ranged from 5×10^{12} to 1×10^{17} Ni cm^{-2}. The current density of the ion beam was less than 1 μA cm^{-2} to minimize beam heating during ion implantation. A part of each plate was shielded from the ion beam by a metal mask to preserve a virgin region as a reference state.

The RBS/channelling technique with a 2 MeV $^4He^+$ ion beam was used to determine the extent of lattice damage and the depth profile of the implanted nickel. The probe ion beam was generated from a 3 MV Van de Graaff accelerator. The backscattered particles were detected by using a surface barrier detector with

0022–2461/86 $03.00 + .12

an energy resolution of 17 keV, placed at a scattering angle of 135° to the incident probe beam.

An Akashi surface profilometer was used to measure the ledge height between the implanted and unimplanted regions.

Hardness measurements using an Akashi microhardness tester were performed with a Knoop profile indenter at a load of 0.24 N. The tests were carried out under ambient conditions at room temperature. Five indentations per specimen were made and the hardness was evaluated from the mean long diagonal value. The hardness values for the implanted region were obtained relative to that for the unimplanted region on the same specimen and were reported as relative values to the unimplanted sapphire. The penetration depth of the indenter tip was $\sim 0.35\,\mu m$, which was about three times deeper than the projected range of the implanted nickel. The hardness value obtained, therefore, mostly represents a composite response of the implanted layer and the underlying unmodified lattice.

The fracture toughness, K_{IC}, of the nickel-implanted surface layer was evaluated by the indentation technique [17]. The radial crack lengths ($2c$) and the indentation diagonals ($2a$) for the Vickers indents produced with loads of 0.49 and 0.98 N were measured under ambient conditions at room temperature and used to calculate apparent fracture-toughness values. Five indentations per load per specimen were made. The crack to indent ratio, c/a, was found to fall in the range $1.2 \leqslant c/a \leqslant 2.3$, and the K_{IC} values were calculated after Niihara *et al.* [18].

Flexural strengths of the nickel-implanted sapphire plates of $7 \times 24 \times 1\,mm^3$ in size were measured at room temperature in three-point flexure with a span of 20 mm and a crosshead speed of $0.05\,cm\,min^{-1}$. The specimens were mounted on an Instron apparatus so that the ion-implanted surface was the tensile side. Five pieces of specimens were tested for a given condition of ion implantation.

In order to obtain the residual surface stress or the volume expansion induced by ion implantation, the cantilever beam technique was employed. The technique [19] measures the deflection of a cantilever beam-shaped specimen, which occurs as a result of stress induced by lattice damage which causes the lattice to expand. Thin sapphire beams of $5 \times 30 \times 0.2\,mm^3$ in size, cut parallel to an {0 0 0 1} plane, were annealed at 1500° C for 6 h in air. The two major surfaces of each beam were coated with an aluminium metal film of about 20 nm. One end of the beam was clamped to a holder and one of the major surfaces of the beam was implanted with 300 keV nickel ions to a dose. After the implantation, the deflection of the free end of the beam was monitored *in situ* by measuring the change of the electrical capacitance of a parallel-plate capacitor formed by the free end and a fixed electrode placed 0.1 mm apart from it. The aluminium metal film coated on the specimen was used as an electrode for forming the gap capacitor and was also used to avoid charge build up at the specimen surface during ion implantation. The implantation and the deflection measurement were repeated successively on the same beam and the deflection was obtained as a function of ion dose.

From the measured deflection of the beam, the integrated stress, S, i.e. the lateral (parallel to the implanted surface) compressive stress integrated over the depth of the damaged layer, was calculated by using the expression [19]

$$S = E\tau^2\delta/3l^2(1 - \sigma), \qquad (1)$$

where δ is the deflection of the beam, τ is the thickness, l is the length of the beam, and E and σ are Young's modulus and Poisson's ratio, respectively. In the calculation, $E = 4.25 \times 10^{12}\,dyn\,cm^{-2}$ and $\sigma = 0.29$ were used [20].

Equation 1 is valid, if $\delta \ll \tau$ [19]. To examine the effect of the beam thickness, the deflection measurement was repeated on a beam 1.0 mm thick. The result agreed well with that obtained with the beam 0.2 mm thick, as shown later in Fig. 3.

3. Results and discussion

3.1. RBS/channelling spectra

In Fig. 1, RBS/channelling spectra for the specimens implanted at 100, 300 and 523 K are compared. Fig. 1a shows the ⟨0 0 0 1⟩ aligned channelling spectra, i.e. the RBS spectra obtained with the probe beam incident parallel to a crystallographic ⟨0 0 0 1⟩ axis, for the specimens implanted with 300 keV nickel ions to various doses at the specimen temperature of 100 K. The random and ⟨0 0 0 1⟩ aligned spectra for an unimplanted specimen are also shown for comparison. From Fig. 1a, it is seen that at a dose of $2 \times 10^{15}\,Ni\,cm^{-2}$, the ⟨0 0 0 1⟩ aligned backscattering yield from aluminium atom reaches the random value in the depth region from ~ 0.5 to $\sim 1.5\,\mu m$. This

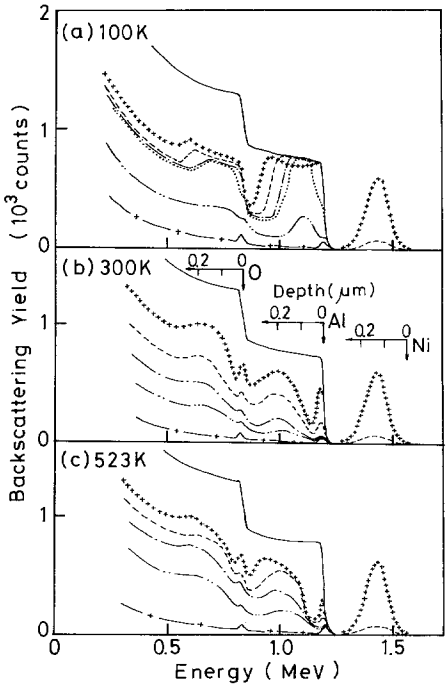

Figure 1 Comparison of RBS/channelling spectra for sapphire implanted with 300 keV nickel ions to various doses at different temperatures. Implantation temperature: (a) 100 K, (b) 300 K, (c) 523 K. Dose: +, $1 \times 10^{17}\,cm^{-2}$; ——, $1 \times 10^{16}\,cm^{-2}$; – · –, $3 \times 10^{15}\,cm^{-2}$; · · · ·, $2 \times 10^{15}\,cm^{-2}$; – · · –, $1 \times 10^{15}\,cm^{-2}$; – + –, unimplanted.

suggests that the subsurface layer is amorphized. Fig. 1a also suggests that with increasing ion dose, the amorphous subsurface layer spreads both upwards and downwards, until it reaches the surface, and that further implantation thickens the amorphous surface layer. A transmission electron microscopy (TEM) study [21] on the surface structure of the specimens implanted with 300 keV nickel ions at 100 K confirmed that a surface amorphous layer was seen in the specimens of 3×10^{15} and 1×10^{17} Ni cm^{-2} and a damaged crystalline layer existed in the specimen of 1×10^{15} Ni cm^{-2}. Thus, from Fig. 1a, the smallest dose required for amorphization, D_a, can be determined to be $D_a \sim 2 \times 10^{15}$ Ni cm^{-2}. The approximate thickness of the amorphous layer can also be evaluated from the figure. For example, at an ion dose of 1×10^{17} Ni cm^{-2}, it is ~270 nm, which is about twice the projected range, R_p, of 300 keV nickel ion in sapphire ($R_p \sim 130$ nm from the RBS experiments). This is also confirmed by the TEM observations [21].

The RBS/channelling spectra for the specimens implanted at 300 and 523 K are shown in Figs. 1b and c, respectively. In these figures, it is seen that the ⟨0 0 0 1⟩ aligned yield for aluminium does not reach the random value even at a high dose of 1×10^{17} Ni cm^{-2}. This shows that in the implantation at room temperature or above, sapphire remains crystalline at least up to a dose of 1×10^{17} Ni cm^{-2}, which is approximately two orders of magnitude larger than D_a at 100 K. These results demonstrate that the extent of lattice damage introduced in sapphire by ion implantation depend strongly on the implantation temperature. Similar results have been reported by White *et al.* [8] for chromium ion implantation in sapphire.

3.2. Volume expansion of amorphized layer

The surface profilometry measurements revealed that the ion-implanted surface was often lifted up compared with the unimplanted surface on the same specimen. In Fig. 2, the step-height observed between implanted and unimplanted area for sapphire implanted with 300 keV nickel ions is plotted as a function of ion dose, D. A clear step could be observed only if sapphire was implanted at 100 K and to a dose of $D > D_a$, at which the formation of an amorphous layer was suggested from the RBS/channelling measurements as described above. For other implantation conditions, the step height was less than 10 nm, the detection limit of the surface profilometer used. These observations suggest that the occurrence of amorphization involves a large expansion of volume. In terms of the step height, Δl, and the initial thickness of the amorphized surface layer, l_0, the volume expansion, $\Delta V/V$, associated with the amorphization is given by $\Delta l/l_0$, if the material expands only in a direction perpendicular to the free surface. The value of l_0 can be approximately estimated from the RBS/channelling spectra, if the energy interval corresponding to the thickness of the amorphous layer is converted to the depth interval by using the density of pure sapphire. $\Delta V/V$ thus estimated is ~30% at an ion dose of 1×10^{17} Ni cm^{-2}. The estimations at lower doses gave similar values of $\Delta V/V$, as shown later in Fig. 4. A similar large increase of volume (20 to 25%) associated with the crystalline to amorphous transformation has been reported by McHargue *et al.* [22], for a single crystal specimen of SiC implanted with chromium ions.

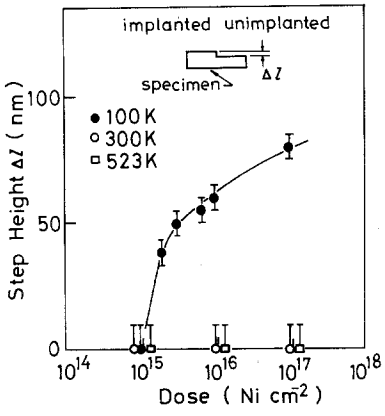

Figure 2 Step height between implanted and unimplanted sapphire areas as a function of ion dose, for the specimen implanted with 300 keV nickel ions at 100, 300 or 523 K.

3.3. Residual compression stress and volume expansion

Sapphire is known to undergo volume expansion when exposed to ion bombardment [16, 23]. This is primarily caused by the introduction of a number of vacancies and interstitial atoms in the host lattice. Because the volume expansion of the implanted-damage layer is restricted by the much thicker underlying undamaged region of the specimen, there yields a lateral compressive stress. In Fig. 3, the integrated lateral stress, S, as a function of ion dose is shown in the dose range $D \leqslant 1 \times 10^{16}$ Ni cm^{-2}, for sapphire implanted with 300 keV nickel ions at either 100 or 300 K. Fig. 3 shows that for the implantation of 300 K, S increases monotonically with dose and shows a broad maximum around $D \sim 5 \times 10^{15}$ Ni cm^{-2}. On the other hand, for the implantation at 100 K, S increases rapidly with dose and reaches a maximum value at $D \sim 1.5 \times 10^{15}$ Ni cm^{-2}, followed by a marked decrease. The marked stress relief is apparently related to the occurrence of amorphization

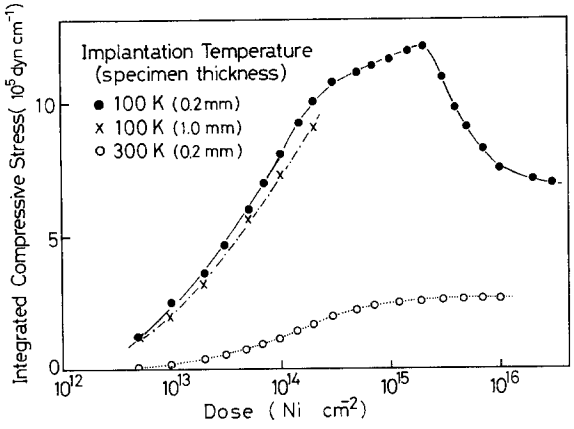

Figure 3 Integrated lateral compressive stress as a function of ion dose for sapphire implanted with 300 keV nickel ions at 100 or 300 K. At 100 K, results are shown for two specimens of different thickness.

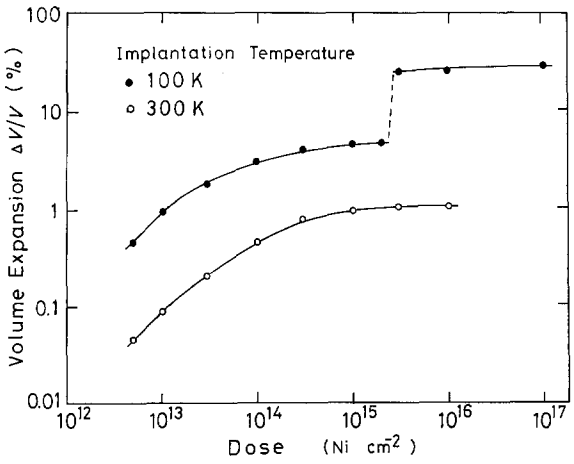

Figure 4 Volume expansion associated with implantation-damage or amorphization as a function of ion dose, for sapphire implanted with 300 keV nickel ions at 100 or 300 K.

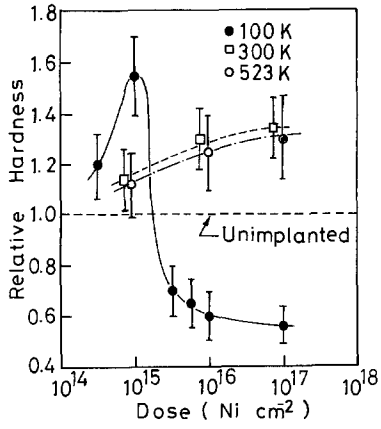

Figure 5 Relative Knoop hardness (implanted to unimplanted) as a function of ion dose for sapphire implanted with 300 keV nickel ions at 100, 300 or 523 K. The load used is 0.24 N.

because the dose at which the stress relief begins agrees well with D_a determined from the RBS/channelling or the surface profilometry measurement.

The implantation-induced lateral stress is thought to be a function of depth and to have a depth distribution similar to that of the lattice damage or the volume density of energy deposited into atomic collisions [23]. The lateral compressive stress averaged over the damaged lattice, T, is found approximately by dividing the integrated stress, S, by the ion projected range, R_p. It should be noted that the lateral stress induced at 100 K is much larger than that at 300 K particularly at doses lower than D_a. For example, the maximum average compressive stress, T_{max}, which is given by S_{max}/R_p, reaches a value of ~ 9 GPa, when the implantation is performed at 100 K, where the maximum integrated stress $S_{max} = 1.2 \times 10^6$ dyn cm^{-1} at $D \sim 1.5 \times 10^{15}$ Ni cm^{-2}. On the other hand, $T_{max} \sim 2$ GPa at 300 K, where $S_{max} = 2.5 \times 10^5$ dyn cm^{-1} at $D \sim 5 \times 10^{15}$ Ni cm^{-2}. Thus, the implantation at a lower temperature is more effective to induce a larger compressive stress.

The volume expansion, $\Delta V/V$, that would occur if the damaged layer were free to expand in all three dimensions is approximately given by

$$\Delta V/V = 3\frac{(1-\sigma)}{E}T \sim 3\frac{(1-\sigma)}{E}\frac{S}{R_p} \quad (2)$$

In Fig. 4, $\Delta V/V$ obtained from the measured values of S by using Equation 2 is plotted as a function of ion dose, where E and σ for the damaged lattice are assumed to be equal to the unimplanted values. The dependences of E and σ on temperature can be neglected at temperatures lower than 300 K [24]. For the implantation conditions where amorphization occurs, the assumption used above is inappropriate, because the Young's modulus of the amorphized layer will be considerably reduced from the value of pure sapphire. In Fig. 4, the values of $\Delta V/V$ obtained in the manner described in the preceding section are shown for doses $D > D_a$ in the implantation at 100 K. Fig. 4 shows that the implantation at 100 K results in a larger expansion of volume or higher concentration of lattice defects than does the implantation at 300 K. This fact indicates that the lattice defects produced by the implantation at 100 K are stabilized and a high concentration of lattice defects can be obtained at a low dose, whereas in the implantation at 300 K and above, considerable annealing of defects occurs during implantation.

3.4. Hardness

In Fig. 5, the variation in microhardness is shown as a function of ion dose for the specimens implanted with 300 keV nickel ions to various doses, at 100, 300 or 523 K. Upon implantation at 100 K, the relative hardness increases up to ~ 1.5 with dose, followed by a rapid decrease around $D \sim D_a$, and then it reaches ~ 0.6. This behaviour of hardness is similar to that observed by White *et al.* [8] in sapphire implanted with chromium ions at 77 K. The hardness increase in $D < \sim 1 \times 10^{15}$ Ni cm^{-2} may be attributed to radiation hardening and the hardness reduction in $D > D_a$ apparently results from the formation of amorphous layer. The thickness of the amorphous layer at an ion dose of 1×10^{17} Ni cm^{-2} is ~ 0.8 relative to the penetration depth of the indenter tip. Therefore, the measured hardness at this dose largely reflects the response of the implanted layer only, and the hardness of the amorphous phase is determined to be ~ 0.6 relative to the unimplanted crystalline phase.

By the implantation at 300 or 523 K, the hardness increased monotonically with dose in the whole dose range investigated. At a high dose such as 1×10^{17} Ni cm^{-2}, solid solution hardening or precipitation hardening as well as radiation hardening may contribute to the observed hardening because of the increased concentration of the implanted nickel. It is interesting to note that the largest increase in hardness is obtained for the implantation condition where the largest compressive stress is induced, as seen from Figs. 3 and 5. This seems to indicate that the increased resistance to the dislocation motion by the introduction of lattice defects is further enhanced by increasing the stress or strain field around the defects. Fig. 5 demonstrates that by nickel implantation at 100 K the hardness of sapphire can be controlled over a wide range.

In Fig. 6, the scanning electron micrographs (SEM) are compared for the 0.24 N Knoop indentations of

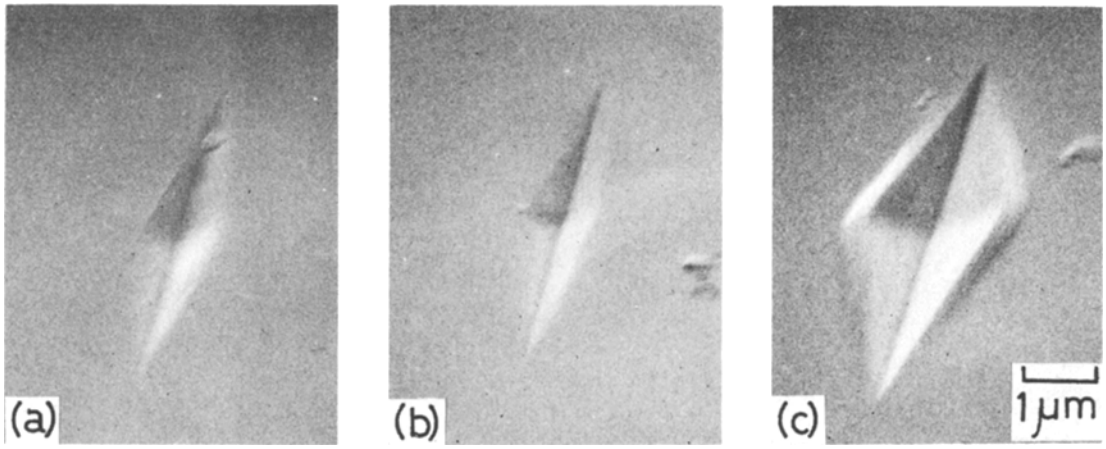

Figure 6 High tilt (75°) SEM images of 0.24 N Knoop indentations in sapphire specimens (a) unimplanted, and implanted with 300 keV nickel ions to a dose of 1×10^{17} Ni cm^{-2} at a specimen temperature of either (b) 523 K or (c) 100 K.

the sapphire specimens unimplanted and implanted with nickel ions to a dose of 1×10^{17} Ni cm^{-2} either at 100 or 523 K. A large ridge around the Knoop indentation can be seen only in the specimen implanted at 100 K. A ridge, although not so large as that at 1×10^{17} Ni cm^{-2}, could also be seen in the specimen implanted to 3×10^{15} Ni cm^{-2} at 100 K. These observations show that the amorphization involves a considerable increase in plasticity. A similar ridge around indentations has been reported by Burnett and Page in sapphire implanted with yttrium ions to very high doses at ambient temperature [6].

3.5. Fracture toughness

In Fig. 7, the fracture toughnesses, K_{IC}, evaluated by the Vickers indentation method are shown as a function of ion dose for the sapphire specimens implanted with 300 keV nickel ions at 100, 300 and 523 K. Upon nickel implantation at every implantation temperature investigated, K_{IC} was found to increase with dose. The K_{IC} values were dependent on the indenter load and the results obtained with loads of 0.49 and 0.98 N are shown in the figure. The use of the lower load resulted in the higher values of fracture toughness. The dimensions of the Vickers indentations used for evaluating K_{IC} were much larger than the layer thickness altered by the implantation. The indentation diagonal ($2a$) and the radial crack length ($2c$) for the unimplanted specimen were 7.5 and 15 μm for 0.49 N, 10 and 23 μm for 0.98 N. Therefore, the fracture toughness for the implanted layer alone may be much larger than the values shown in Fig. 7. The indentation technique for evaluating K_{IC} requires the generation of cracks, but the use of a load lower than 0.48 N often generated no cracks particularly in the specimens implanted to high doses. It is interesting to note that significant increases of K_{IC} are still found with indenter loads that generate cracks of dimensions much larger than R_p.

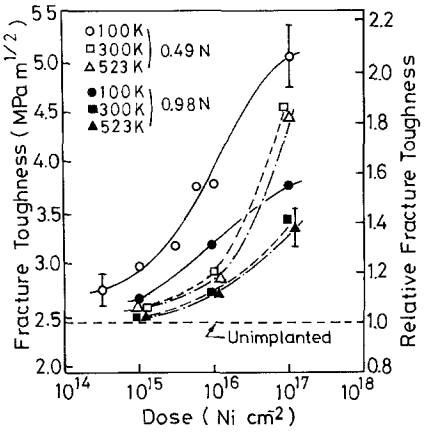

Figure 7 Surface fracture toughness as a function of ion dose for the sapphire implanted with 300 keV nickel ions at 100, 300 or 523 K. The K_{IC} values evaluated from the Vickers indentations at loads of 0.49 and 0.98 N are shown.

Fig. 7 shows that at a given dose the implantation at 100 K is more effective in increasing K_{IC} than that at 300 or 523 K. Because a compressive stress is considered to increase K_{IC}, this result is consistent with the observation that the compressive stress induced by the implantation at 100 K is 3 to 9 times as large as that at 300 K, as shown in Fig. 3. The softening or increased plasticity due to amorphization may also contribute to the fracture-toughness increase. Indeed, for the implantation at 100 K, the increase in K_{IC} at 1×10^{17} Ni cm^{-2} is much larger than that at 1×10^{15} Ni cm^{-2}, though the compressive stress at the former dose is probably about one half of the value at the latter dose. Fig. 7 also shows that at the dose of 1×10^{17} Ni cm^{-2}, which is the highest dose used here, a large increase of K_{IC} is obtained even by the implantation at 300 or 523 K. At 300 or 523 K, sapphire remains crystalline to the dose of 1×10^{17} Ni cm^{-2}, at which the concentration of the implanted nickel amounts to ~20% of the aluminium atomic concentration in pure sapphire. The increased nickel atoms are expected to agglomerate to form clusters and metallic colloids or precipitates during ion implantation. The large increase in K_{IC} may be attributed to this structure as well as to the compressive stress probably of ~2 GPa. Increases in fracture strength and toughness have been found in MgO crystal containing metallic nickel colloids or precipitates [25].

3.6. Flexural strength

The flexural strength of bulk sapphire plates has been

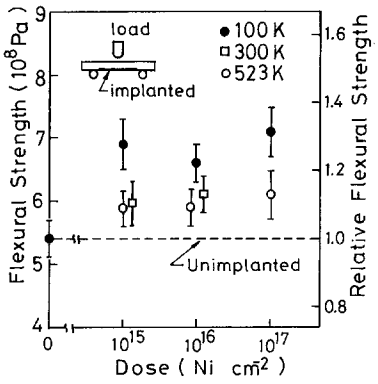

Figure 8 Flexural strength as a function of ion dose for sapphire plates implanted with 300 keV nickel ions at 100, 300 and 523 K.

reported to be significantly increased by ion implantation and the strength increase has been attributed to the surface compressive stress induced by the implantation [5, 7]. Because the compressive stress was found to depend strongly on the implantation temperature as described before, it is interesting to investigate the effects of implantation temperature and surface amorphization on the flexural strength. Fig. 8 shows the dose dependence of flexural strength of sapphire plates implanted with 300 keV nickel ions at 100, 300 and 523 K. As seen in the figure, nickel implantation increases the flexural strength at every dose and implantation temperature investigated. It is also seen that the implantation at 100 K is more effective in increasing the flexural strength than that at 300 or 523 K. These observations may be qualitatively explained by the compressive stress shown in Fig. 3, if we consider that the amount of strengthening increases with increasing compressive stress. Recently, Green [26] has put forward a theoretical approach for predicting the amount of strengthening of materials by an introduction of the surface compressive stress, and has found that the strengthening simply depends on the magnitude of the compressive stress and the ratio, t_1, of the compressive layer depth to flaw size. In particular, when $t_1 > 1$, the strength is simply increased by the amount of the compressive stress. If this was the case for the present study, a strength increase of ~ 9 GPa would be obtained when the specimen is implanted at 100 K to a dose of $\sim 1.5 \times 10^{15}$ Ni cm^{-2}. However, the observed strength increase around this implantation condition is only ~ 0.15 GPa as seen from Fig. 8. The difference suggests that the thickness of the compressive layer is fairly small compared with the size of the surface flaw from which the fracture occurs. The thickness of the compressive layer is about R_p ($\sim 0.13\,\mu$m), whereas the depth of the surface flaw for the sapphire plates used here is probably 1 to 10 μm. When $t_1 < 1$, Green has shown that the strengthening can be increased by increasing the magnitude of the compressive stress and that the extent of strengthening saturates at high values of compressive stress due to partial crack closure. The present experimental results on flexural strength in the dose range $D \leqslant 1 \times 10^{16}$ Ni cm^{-2} can be qualitatively accounted for by the measured compressive stress in the light of theory for $t_1 < 1$.

3.7. Shape change of pre-existing surface flaw by amorphization

The flexural strength increase is largely attributed to the surface compressive stress induced by ion implantation. The occurrence of amorphization results in a relief of the compressive stress accumulated by the preceding ion implantation. It is therefore expected that for the implantation at 100 K, the strength increase is largest at a dose just below D_a, the critical dose for amorphization. However, Fig. 8 shows that the strength increase at 1×10^{17} Ni cm^{-2} is comparable to or even larger than that at 1×10^{15} Ni cm^{-2}, though the compressive stress at the former dose is probably about one half of the value at the latter dose, as expected from Fig. 3. It is thus suggested that the production of a thick amorphous surface layer by ion implantation also contributes to increase the flexural strength. A possible mechanism for this strengthening may be a reduction of the stress-concentration at the tip of the surface flaw that determines the strength. The large volume expansion associated with the amorphization is expected to change the shape and size of pre-existent surface flaws and hence the extent of stress concentrations at the flaws under an applied external stress.

To investigate the effect of amorphization on the shape of a surface flaw, the sapphire plates were preindented with a Knoop-profile indenter at a load of 1.96 N and were implanted with 300 keV nickel ions to a dose of 1×10^{17} Ni cm^{-2} at 100 and 523 K. The long diagonal and the depth of the Knoop indentation before implantation were 40 and 1.4 μm, respectively. In Fig. 9, the SEM images of the Knoop indentation flaw before and after the implantations were compared. After the implantation at 100 K, a remarkable blunting of the Knoop flaw is seen, and both the diagonal and the depth of the Knoop indentation appear to become smaller. On the other hand, by the implantation at 523 K to the same dose, the appearance of the Knoop flaw is hardly changed from the unimplanted one. The shape change of the Knoop flaw is apparently related to the amorphization that only occurs in the low-temperature implantation. The ion sputtering effect may also cause a surface morphological change. The sputtering yield for Al_2O_3 by the bombardment with 300 keV nickel ions and its dependence on the substrate temperature are not known. However, the ion sputtering effect would not explain the observed dependence of the shape change on implantation temperature, because sputtering yield generally increases or changes little with the substrate temperature particularly in the temperature range of the present investigation [27]. Thus, it is concluded that the remarkable change in the apparent shape and size of the Knoop flaw dominantly arises from the surface amorphization. The large volume expansion associated with the amorphization should dull the edges and tips of surface flaws or cracks and even close open cracks in their near-surface part, and therefore should reduce the stress concentrations at the surface flaws when an external tensile stress is applied. These effects will be more remarkable as the amorphous surface layer thickens with increasing ion dose and

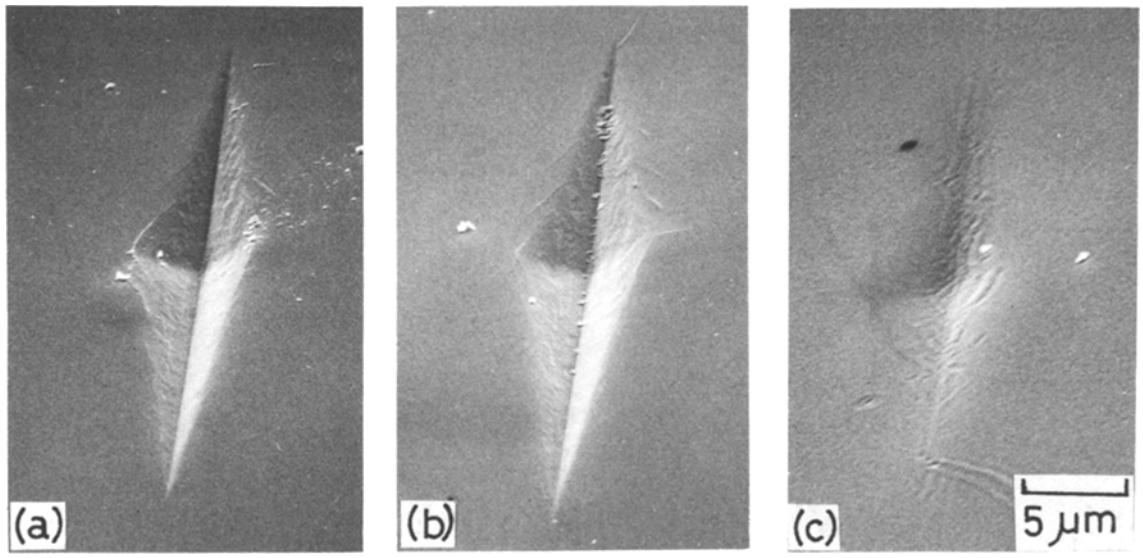

Figure 9 High tilt (75°) SEM images showing the change in appearance of a pre-indented 1.96 N Knoop indentation by nickel ion implantation. (a) Before implantation, and after implanting 300 keV nickel ions to a dose of 1×10^{17} Ni cm^{-2} at a temperature of either (b) 523 K, or (c) 100 K.

are considered to partly explain the comparatively large increase in the flexural strength at the dose of 1×10^{17} Ni cm^{-2} in the implantation at 100 K.

4. Conclusions

By implanting nickel ions at a low temperature (100 K) and at room temperature (300 K) and above (523 K), the changes of the mechanical properties of sapphire caused by the implantation have been demonstrated to depend strongly on implantation temperature as follows:

1. Hardness can be varied with ion dose over a wider range by the low-temperature implantation. For 300 keV nickel ions, the relative hardness ranged from ~ 0.6 to ~ 1.5 by the implantation at 100 K, whereas at 300 or 523 K, it ranged from 1.0 to ~ 1.3.

2. Both surface fracture toughness and bulk flexural strength are increased by ion implantation, and at a given dose the low temperature implantation is more effective in increasing both of them.

3. The low-temperature implantation induced a surface compressive stress three to nine times larger than that obtained by implanting at room temperature to the same dose. This difference in the residual compressive stress largely accounts for the dependence of the mechanical properties on the implantation temperature particularly for the implantation condition at which sapphire remains crystalline.

4. A surface amorphization can be easily obtained by the low-temperature implantation. The dose required for the amorphization at 100 K was $\sim 2 \times 10^{15}$ Ni cm^{-2}, whereas at 300 K and above sapphire remained crystalline at least up to a dose of 1×10^{17} Ni cm^{-2}. The amorphous layer showed a significant softening and increased plasticity. The amorphization was also suggested to result in an increase in surface fracture toughness.

5. The amorphization involves a large volume expansion of $\sim 30\%$. This effect has been demonstrated to change considerably the apparent shape and size of pre-existing surface flaws and suggested to increase the flexural strength by decreasing the stress concentrations at the surface flaws under an applied external tensile stress.

Acknowledgements

We would like to thank Drs Y. Kido and S. Kobayashi for discussions.

References

1. C. J. McHARGUE, H. NARAMOTO, B. R. APPLETON, C. W. WHITE and J. M. WILLIAMS, *Proc. Mater. Res. Soc.* **7** (1982) 147.
2. H. NARAMOTO, C. W. WHITE, J. M. WILLIAMS, C. J. McHARGUE, O. W. HOLLAND, M. M. ABRAHAM and B. R. APPLETON, *J. Appl. Phys.* **54** (1983) 683.
3. C. J. McHARGUE and C. S. YUST, *J. Amer. Ceram. Soc.* **67** (1984) 117.
4. G. C. FARLOW, C. W. WHITE, C. J. McHARGUE and B. R. APPLETON, *Proc. Mater. Res. Soc.* **27** (1984) 395.
5. T. HIOKI, A. ITOH, S. NODA, H. DOI, J. KAWAMOTO and O. KAMIGAITO, *J. Mater. Sci. Lett.* **3** (1984) 1099.
6. P. J. BURNETT and T. J. PAGE, *J. Mater. Sci.* **19** (1984) 3524.
7. T. HIOKI, A. ITOH, S. NODA, H. DOI, J. KAWAMOTO and O. KAMIGAITO, *Nucl. Inst. Meth. Phys. Res.* **B7/8** (1985) 521.
8. C. W. WHITE, G. C. FARLOW, C. J. McHARGUE, P. S. SKLAD, M. P. ANGELINI and B. R. APPLETON, *ibid.* **B7/8** (1985) 473.
9. S. G. ROBERTS and T. F. PAGE, in "Ion Implantation into Metals", edited by V. Ashworth, W. A. Grant and R. P. M. Proctoer (Pergamon, Oxford, 1982) p. 135.
10. C. J. McHARGUE and J. M. WILLIAMS, *Proc. Mater. Res. Soc.* **7** (1982) 303.
11. J. M. WILLIAMS, C. J. McHARGUE and B. R. APPLETON, *Nucl. Inst. Meth.* **202/210** (1983) 1159.
12. J. K. COCHRAN, K. O. LEGG and G. R. BALDAU, in "Emergent Process Methods for High Technology Ceramics", edited by R. Davis, H. Palmour and R. Porter (Plenum, New York, 1984) p. 549.
13. K. O. LEGG, J. K. COCHRAN Jr, H. F. SOLNICK-LEGG and X. L. MANN, *Nucl. Inst. Meth. Phys. Res.* **B7/8** (1985) 535.
14. H. HASEGAWA, T. HIOKI and O. KAMIGAITO, *J. Mater. Sci. Lett.* **4** (1985) 1092.

15. P. J. BURNETT and T. F. PAGE, *Proc. Mater. Res. Soc.* **27** (1984) 401.
16. G. W. ARNOLD, G. B. KREFFT and C. B. NORRIS, *Appl. Phys. Lett.* **25** (1974) 540.
17. A. G. EVANS and E. A. CHARLES, *J. Amer. Ceram. Soc.* **59** (1976) 371.
18. K. NIIHARA, R. MORENA and P. H. HASSELMAN, *J. Mater. Sci. Lett.* **1** (1982) 13.
19. E. P. EERNISSE, *Appl. Phys. Lett.* **18** (1971) 581.
20. J. H. GIESKE and G. R. BARSCH, *Phys. Status Solidi* **29** (1968) 581.
21. S. KOBAYASHI, T. HIOKI and O. KAMIGAITO, to be published.
22. C. J. McHARGUE, C. W. WHITE, B. R. APPLETON, G. C. FARLOW and J. M. WILLIAMS, *Proc. Mater. Res. Soc.* **27** (1984) 385.
23. G. B. KREFFT and E. P EERNISSE, *J. Appl. Phys.* **48** (1977) 9.
24. J. B. WACHTMAN Jr, W. E. TEFFT, D. G. LAM Jr and C. S. APSTEIN, *Phys. Rev.* **122** (1961) 1754.
25. J. NARAYAN, Y. CHEN and R. M. MOON, *Proc. Mater. Res. Soc.* **24** (1984) 101.
26. D. J. GREEN, *J. Mater. Sci.* **19** (1984) 2165.
27. J. M. FLUIT, C. SNOEK and J. KISTEMAKER, *Physica* **30** (1964) 144.

Received 30 April
and accepted 12 June 1985